

0024 806 3708 4700  
C. 2

0066326



TECH LIBRARY KAFB, NM

# NATIONAL ADVISORY COMMITTEE FOR AERONAUTICS

TECHNICAL NOTE 3708

INVESTIGATION AT SUPERSONIC SPEEDS OF THE VARIATION WITH  
REYNOLDS NUMBER AND MACH NUMBER OF THE TOTAL, BASE,  
AND SKIN-FRICTION DRAG OF SEVEN BOATTAIL BODIES  
OF REVOLUTION DESIGNED FOR MINIMUM WAVE DRAG

By August F. Bromm, Jr., and Julia M. Goodwin

Langley Aeronautical Laboratory  
Langley Field, Va.



Washington

June 1956

APR 1956



0066326

## TECHNICAL NOTE 3708

INVESTIGATION AT SUPERSONIC SPEEDS OF THE VARIATION WITH  
REYNOLDS NUMBER AND MACH NUMBER OF THE TOTAL, BASE,  
AND SKIN-FRICTION DRAG OF SEVEN BOATTAIL BODIES  
OF REVOLUTION DESIGNED FOR MINIMUM WAVE DRAG<sup>1</sup>

By August F. Bromm, Jr., and Julia M. Goodwin

## SUMMARY

An investigation has been conducted in the Langley 9-inch supersonic tunnel to determine the effect of the variation with Reynolds number and Mach number of the total, base, and skin-friction drag at zero lift of seven boattail bodies of revolution designed for minimum wave drag according to NACA Technical Note 2550. The investigation covered a Reynolds number range from approximately  $1.0 \times 10^6$  to  $10.0 \times 10^6$  at Mach numbers of 1.62, 1.93, and 2.41, respectively. The results show that base drag and, in general, the total drag increase with increasing values of the ratio of base area to maximum area  $B/S_{\max}$ , although the results reported in NACA Technical Note 3054 showed that the wave drag decreased with increasing values of  $B/S_{\max}$ . The laminar skin-friction drag is in agreement with the theoretical predictions used, and, within the Mach number range of these tests, the simple Blasius incompressible theory gives a satisfactory prediction. Except for values of  $B/S_{\max}$  near 1, the Reynolds number of transition increases with increasing Mach number and, as this ratio approaches 1, this variation is seen to reverse. These variations in Reynolds number of transition with Mach number appear to be associated with the changes in pressure gradient over the rear of the bodies.

## INTRODUCTION

Considerable interest exists at the present time in the drag characteristics at supersonic speeds of nonlifting bodies of revolution designed for minimum wave drag. One such family of boattail bodies, having shapes determined by the method of reference 1, has been investigated in reference 2 to assess the effect of Reynolds number and Mach number upon the

<sup>1</sup>Supersedes declassified NACA Research Memorandum L53I29b by August F. Bromm, Jr., and Julia M. Goodwin, 1953.

wave-drag characteristics. In order to find body profiles which have minimum total drag, the base-pressure drag and the skin-friction drag must also be considered. For example, if the configuration to be considered has a supersonic jet occupying most of the base area, the base-pressure drag may be neglected, but if no jet exists at the body base, base drag becomes an important factor in determining whether the body profile considered has a minimum total drag. Thus, the purpose of this investigation is to provide information concerning the total, base, and skin-friction drag of the seven boattail bodies of revolution of reference 2.

The investigation was conducted in the Langley 9-inch supersonic tunnel over a Reynolds number range from approximately  $1.0 \times 10^6$  to  $10.0 \times 10^6$  at Mach numbers of 1.62, 1.93, and 2.41, respectively.

#### SYMBOLS

$S_{\max}$	maximum cross-sectional area of body
$B$	base area
$C_{DT}$	total-drag coefficient, $\frac{\text{Total drag}}{q_o S_{\max}}$
$C_{Db}$	base-drag coefficient, $P_b \frac{B}{S_{\max}}$
$C_{Dw}$	wave-drag coefficient, $\int_0^l P \frac{d}{dx} \left( \frac{r}{r_{\max}} \right)^2 dx$
$C_{Df}$	average skin-friction-drag coefficient, $C_{DT} - (C_{Db} + C_{Dw})$
$l$	body length
$r$	local body radius
$r_{\max}$	maximum body radius
$x$	distance from nose measured along body axis
$C_f$	skin-friction coefficient

P	pressure coefficient, $\frac{p_l - p_o}{q_o}$
$P_b$	base pressure coefficient
$p_o$	free-stream static pressure
$p_l$	local static pressure
$q_o$	free-stream dynamic pressure, $\frac{\gamma}{2} p_o M_o^2$
$M_o$	free-stream Mach number
R	Reynolds number based on body length and free-stream conditions
$R_t$	Reynolds number of transition
$\gamma$	ratio of specific heats for air, 1.4

#### APPARATUS

##### Wind Tunnel

The Langley 9-inch supersonic tunnel is a continuous-operation, closed-circuit type of wind tunnel in which the pressure, temperature, and humidity of the enclosed air can be regulated. Different test Mach numbers are provided by interchangeable nozzle blocks which form test sections approximately 9 inches square. Eleven fine-mesh turbulence-damping screens are installed in the relatively large-area settling chamber ahead of the supersonic nozzle. The turbulence level of the tunnel is considered low, based on the turbulence-level measurements presented in reference 3. A schlieren optical system is provided for qualitative flow observations.

##### Models

A drawing illustrating the construction details of the models and giving the pertinent dimensions is shown in figure 1, and a photograph of the models is shown in figure 2. These are the same models which were

employed in the tests of reference 2. The seven body shapes were determined from the following general equation given in reference 1:

$$S(x') = \frac{B'}{\pi c} \sqrt{1 - x'^2} + \frac{B'}{\pi c} \frac{(x' - c)^2}{\sqrt{1 - c^2}} \log_e N + \frac{B'}{\pi} \cos^{-1}(-x')$$

where

$S(x')$       nondimensional body cross-sectional area,

$$\pi \frac{r(x')^2}{(l/2)^2}$$

$B'$       base area of body divided by  $(l/2)^2$

$x'$       distance made nondimensional with respect to  $l/2$  and measured along body axis from midpoint of body

$c$       distance, divided by  $l/2$ , from midpoint of body to location of maximum area

$$N = \frac{1 - cx' - \sqrt{1 - c^2} \sqrt{1 - x'^2}}{|x' - c|}$$

All the models had a fineness ratio of 8 and varied in ratio of base area to maximum area from about 0.1 to 1.0. The models were manufactured from stainless steel and were carefully polished throughout the tests to preserve a uniformity of surface conditions. The surface roughness was of the order of 8 rms microinches. An internal strain-gage balance, described subsequently, was used to measure the total drag. The base-pressure measurements were obtained from two pressure tubes extending a short distance into the hollow sting. This hollow sting served as a conduit for the strain-gage wires and was sealed at the support end of the sting and vented to the chamber within the model; thus, the pressure measured was for all practical purposes the base pressure of the models.

#### Balance

The balance used in this investigation and a typical installation are shown in figure 3. The balance is a strain-gage type consisting of two flex beams and two restraining and measuring beams. Since interaction in the balance was found to be negligible, the two restraining and measuring beams measure only the chord force.

## TESTS

All tests were conducted at Mach numbers of 1.62, 1.93, and 2.41 and over a Reynolds number range from approximately  $1.0 \times 10^6$  to  $10.0 \times 10^6$  at each Mach number. The temperature range of the tests was from approximately 75° F to 135° F. Throughout the tests the dew-point was kept sufficiently low to insure negligible effects of condensation. A condition of zero pitch and yaw with respect to the tunnel side walls and center line, respectively, was maintained as closely as possible. Optical means were used to check model yaw and pitch. Throughout the entire test program the models were under schlieren observation. A constant check of the strain-gage-balance calibration was also maintained during the tests.

## PRECISION OF DATA

All models were maintained within  $\pm 0.15^\circ$  of zero pitch and yaw with respect to the tunnel side walls and center line, respectively. Previous measurements of the flow angularity in the tunnel test section have shown negligible deviations. The estimated accuracies of the test variables and the measured coefficients are given in the following table for a tunnel stagnation pressure of 30 in. Hg corresponding to a Reynolds number of approximately  $2.5 \times 10^6$ :

Mach number, M . . . . .	$\pm 0.01$
Reynolds number per inch, R . . . . .	$\pm 0.004 \times 10^6$
Total-drag coefficient, $C_{D_T}$ . . . . .	$\pm 0.003$
Base-drag coefficient, $C_{D_b}$ . . . . .	$\pm 0.002$
Average skin-friction-drag coefficient . . . . .	$\pm 0.004$

## RESULTS AND DISCUSSION

## Total and Base Drag

The results of the total-drag measurements and the simultaneous base-pressure measurements are presented in figures 4 and 5 as total-drag coefficient and base-drag coefficient. For models 3 to 7, the ratio of sting diameter to base diameter is sufficiently small to have negligible effects on the values of base drag; however, for models 1 and 2, this ratio becomes marginal or excessive to the extent that the base-pressure measurements must be considered indicative of order of magnitude only. This sting

interference upon the base pressure for models 1 and 2 would contribute only small errors to the total-drag measurements.

The total drag for models 4 to 7 (fig. 4) increases with increasing Reynolds number in the low Reynolds number range because of the abrupt increase in base drag caused by wake transition. In general, for models 1, 2, and 3 (fig. 4), the total drag decreases with increasing Reynolds number in the low Reynolds number range. This difference in variation of total drag with Reynolds number is probably due to separation effects on the rear portion of these bodies and to the effects of a large ratio of sting diameter to base diameter. As Reynolds number increases beyond about  $2 \times 10^6$ , the variation for all models is fairly constant until the Reynolds number is reached for which the abrupt decrease in base drag is realized. The steady rise in total drag that takes place after this decrease is essentially the increase in skin-friction drag caused by the forward movement along the body of the point of natural transition. Similar trends in the variation of total drag with Reynolds number are shown in references 3 and 4 except that, because of differences in body shape and wake transition, the abrupt rise in total drag occurs at higher Reynolds numbers.

In the low Reynolds number range the rapid increase in base drag is due to wake transition as explained in references 3 and 5. As the point of transition in the wake moves toward the base of the body, the base drag increases to a peak value. Beyond the peak value there is an abrupt decrease in base drag which becomes less apparent as the ratio of base area to maximum area  $B/S_{\max}$  decreases and as the Mach number increases. This decrease in base drag occurs as the point of transition moves onto the body surface just ahead of the body base. With an increase in Reynolds number beyond that for transition on the body surface, the base-drag variation is small.

In previous tests (ref. 2) of the same bodies tested in this investigation it was seen that the magnitude of the wave-drag coefficient  $C_{Dw}$  decreased with increasing ratio of base area to maximum area  $B/S_{\max}$ . From the present tests, this beneficial effect upon the wave drag from increasing  $B/S_{\max}$  is found to be overshadowed by the large increase in base drag. This increase in base drag is sufficient to cause the total drag to exhibit, in general, a large increase with increasing  $B/S_{\max}$ . Thus, it is important to consider whether total or wave drag is the governing criterion in selecting a body from this family. For a jet exhausting from the base and having an exit area covering most of the base area, the wave drag might be the logical basis for selection.

## Skin-Friction Drag

The values of skin-friction-drag coefficient determined from the force and base-pressure measurements of the present investigation and from the wave-drag results of reference 2 are presented in figure 6. The values of wave drag below a Reynolds number of approximately  $2 \times 10^6$  were determined by extrapolation. Below a Reynolds number of  $1 \times 10^6$  the comparatively few values of skin-friction drag were of little importance in assessing the agreement with theory and have been omitted. The Frankl-Voishel extended theory for turbulent flow at  $M = 2.41$  (ref. 6) was used as a reference level in figure 6. For comparison with the experimental results for laminar flow over the entire body, two methods for predicting laminar skin-friction drag were used. The first of these methods was the incompressible Blasius relation (with the Töpfer constant) in which

$$C_F = \frac{1.328}{\sqrt{R}}$$

The second method was that of Chapman and Rubesin in which

$$C_F = \frac{1.328}{\sqrt{R}} \sqrt{C}$$

where the constant  $C$  is dependent upon Mach number and is determined as shown in reference 7. The Chapman and Rubesin estimate has been calculated only for  $M = 2.41$  since the predictions for the other two Mach numbers would lie between this estimate and the Blasius incompressible prediction. Both of these theoretical methods are for a flat plate with zero pressure gradient and zero heat transfer. The skin-friction drag predicted by references 6 and 7 and the Blasius relation (fig. 6) are based on the maximum area of the models.

The accuracy of the experimental results does not permit an evaluation of such small differences as are exhibited between the theoretical predictions. Thus, it would seem permissible to say that within the accuracy of this investigation the simple Blasius incompressible theory for a flat plate gives a satisfactory prediction of laminar skin-friction drag. At  $M = 2.41$ , all the experimental results indicate a more rapid decrease in laminar skin friction with increasing Reynolds number than that predicted by the theoretical results. This condition also occurs at  $M = 2.41$  for the parabolic body (NACA RM-10) of reference 3.



### Reynolds Number of Transition

Figure 7 presents the variation of Reynolds number of transition  $R_t$  with the ratio of base area to maximum area  $B/S_{max}$  at  $M = 1.62$ ,  $1.93$ , and  $2.41$ . The values of  $R_t$  were picked from the skin-friction-drag curves (fig. 6). Since the transition occurred at the base of the bodies on only three of the models at  $M = 2.41$ , the transition points for the other four models were picked from the skin-friction-drag curves as being no lower than those shown in figure 7. These points are indicated by flagged symbols. Another method of obtaining values of  $R_t$  is by use of the base-pressure data. Several investigations (see refs. 3, 5, and 8, for example) have shown that base-pressure data may be used to determine values of  $R_t$  in many cases; the present base-drag results show that a very good check can be made of the majority of the values of  $R_t$  taken from the skin-friction-drag curves.

The variation of the maximum adverse pressure gradient with the ratio of base area to maximum area at  $M = 1.62$ ,  $1.93$ , and  $2.41$  is presented in figure 8. The pressure-gradient values were obtained from the pressure-distribution curves of reference 2.

The Reynolds number of transition is seen to vary with  $B/S_{max}$  in the same manner as the maximum adverse pressure gradient. This agreement in trend appears indicative of the reason for the variation of  $R_t$  with Mach number for values of  $B/S_{max}$  less than 1. The recompression of the flow over the base of the boattail bodies is seen ( $B/S_{max} < 1$ ) to cause increasingly adverse pressure gradients with decreasing Mach number, as would be expected. It appears that the effects of these adverse pressure gradients overshadow the direct effects of increasing Mach number upon  $R_t$  (i.e., for zero pressure gradient) within this Mach number range; consequently, except when  $B/S_{max}$  approaches 1,  $R_t$  increases with increasing Mach number. When  $B/S_{max}$  approaches 1, the reversal in the variation of  $R_t$  with Mach number is probably due to the decrease and, finally, the elimination of the adverse gradients.

### CONCLUSIONS

An investigation has been conducted in the Langley 9-inch supersonic tunnel to determine the effect of the variation with Reynolds number and Mach number of the total, base, and skin-friction drag at zero lift of seven boattail bodies of revolution designed for minimum wave drag according

to NACA Technical Note 2550. The tests covered a Reynolds number range from approximately  $1.0 \times 10^6$  to  $10.0 \times 10^6$  at Mach numbers of 1.62, 1.93, and 2.41, respectively. The following conclusions are indicated:

1. Although the results of NACA Technical Note 3054 showed that the wave drag of the same bodies tested in the present investigation decreased with increasing values of the ratio of base area to maximum area  $B/S_{\max}$ , the present results show that the base drag and, in general, the total drag increase with increasing values of  $B/S_{\max}$ .

2. Within the experimental accuracy of these tests, the laminar skin-friction drag of these bodies is in agreement with the theoretical predictions, and within this Mach number range the simple Blasius incompressible theory for a flat plate gives a satisfactory prediction.

3. Except for values of  $B/S_{\max}$  near 1, the Reynolds number of transition increases with increasing Mach number and, as this ratio approaches 1, this variation is seen to reverse. These variations in Reynolds number of transition with Mach number appear to be associated with the changes in the pressure gradients over the rear of the bodies.

Langley Aeronautical Laboratory,  
National Advisory Committee for Aeronautics,  
Langley Field, Va., September 17, 1953.

## REFERENCES

1. Adams, Mac C.: Determination of Shapes of Boattail Bodies of Revolution for Minimum Wave Drag. NACA TN 2550, 1951.
2. Bromm, August F., Jr., and Goodwin, Julia M.: Investigation at Supersonic Speeds of the Wave Drag of Seven Boattail Bodies of Revolution Designed for Minimum Wave Drag. NACA TN 3054, 1953.
3. Love, Eugene S., Coletti, Donald E., and Bromm, August F., Jr.: Investigation of the Variation With Reynolds Number of the Base, Wave, and Skin-Friction Drag of a Parabolic Body of Revolution (NACA RM-10) at Mach Numbers of 1.62, 1.93, and 2.41 in the Langley 9-Inch Supersonic Tunnel. NACA RM L52H21, 1952.
4. Czarnecki, K. R., and Marte, Jack E.: Skin-Friction Drag and Boundary-Layer Transition on a Parabolic Body of Revolution (NACA RM-10) at a Mach Number of 1.6 in the Langley 4- by 4-Foot Supersonic Pressure Tunnel. NACA RM L52C24, 1952.
5. Love, Eugene S., and O'Donnell, Robert M.: Investigations at Supersonic Speeds of the Base Pressure on Bodies of Revolution With and Without Sweptback Stabilizing Fins. NACA RM L52J21a, 1952.
6. Rubesin, Morris W., Maydew, Randall C., and Varga, Steven A.: An Analytical and Experimental Investigation of the Skin Friction of the Turbulent Boundary Layer on a Flat Plate at Supersonic Speeds. NACA TN 2305, 1951.
7. Chapman, Dean R., and Rubesin, Morris W.: Temperature and Velocity Profiles in the Compressible Laminar Boundary Layer With Arbitrary Distribution of Surface Temperature. Jour. Aero. Sci., vol. 16, no. 9, Sept. 1949, pp. 547-565.
8. Potter, J. L.: Friction Drag and Transition Reynolds Number on Bodies of Revolution at Supersonic Speeds. NAVORD Rep. 2150, U. S. Naval Ord. Lab., White Oak, Md., Aug. 20, 1951.

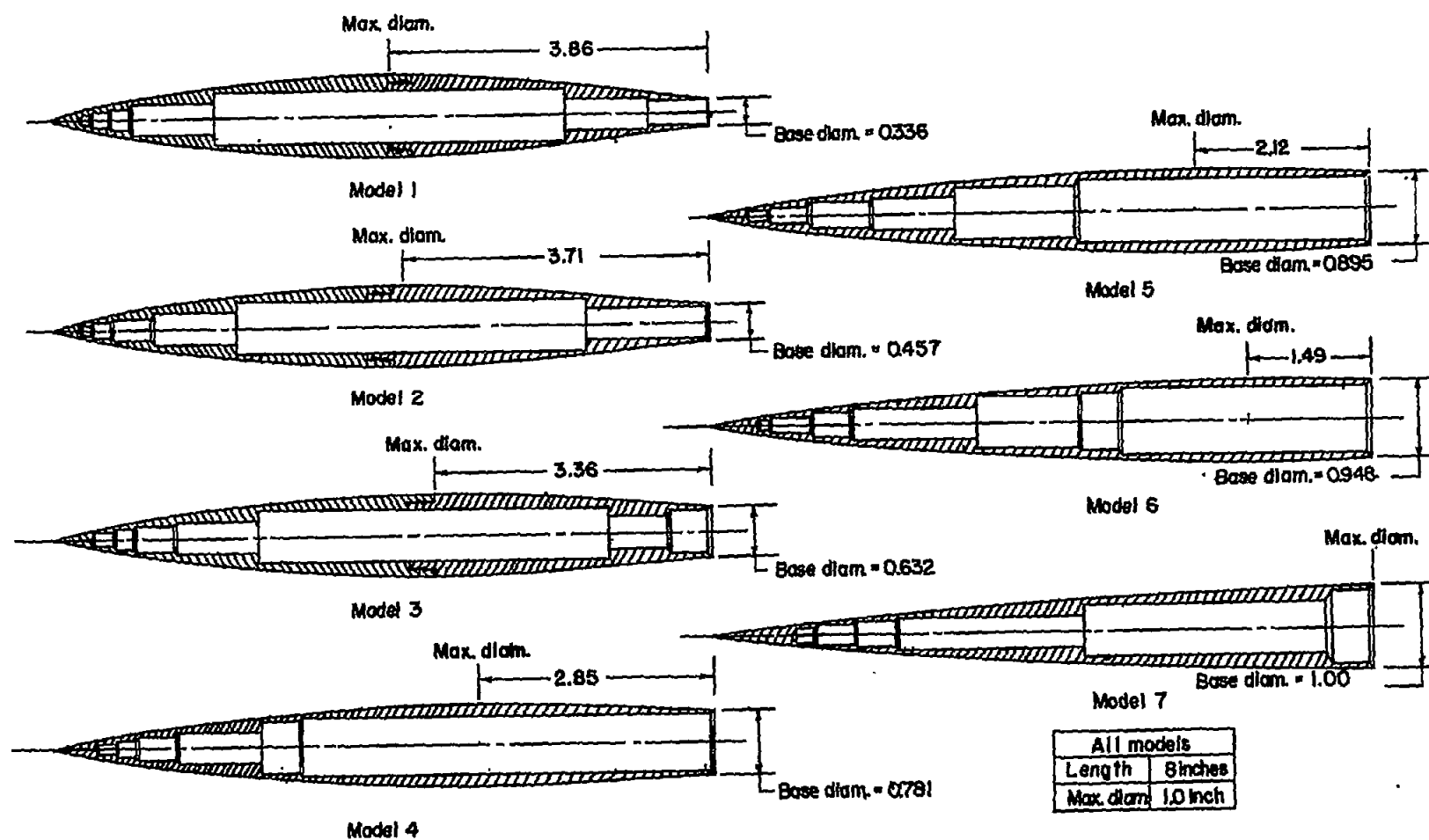
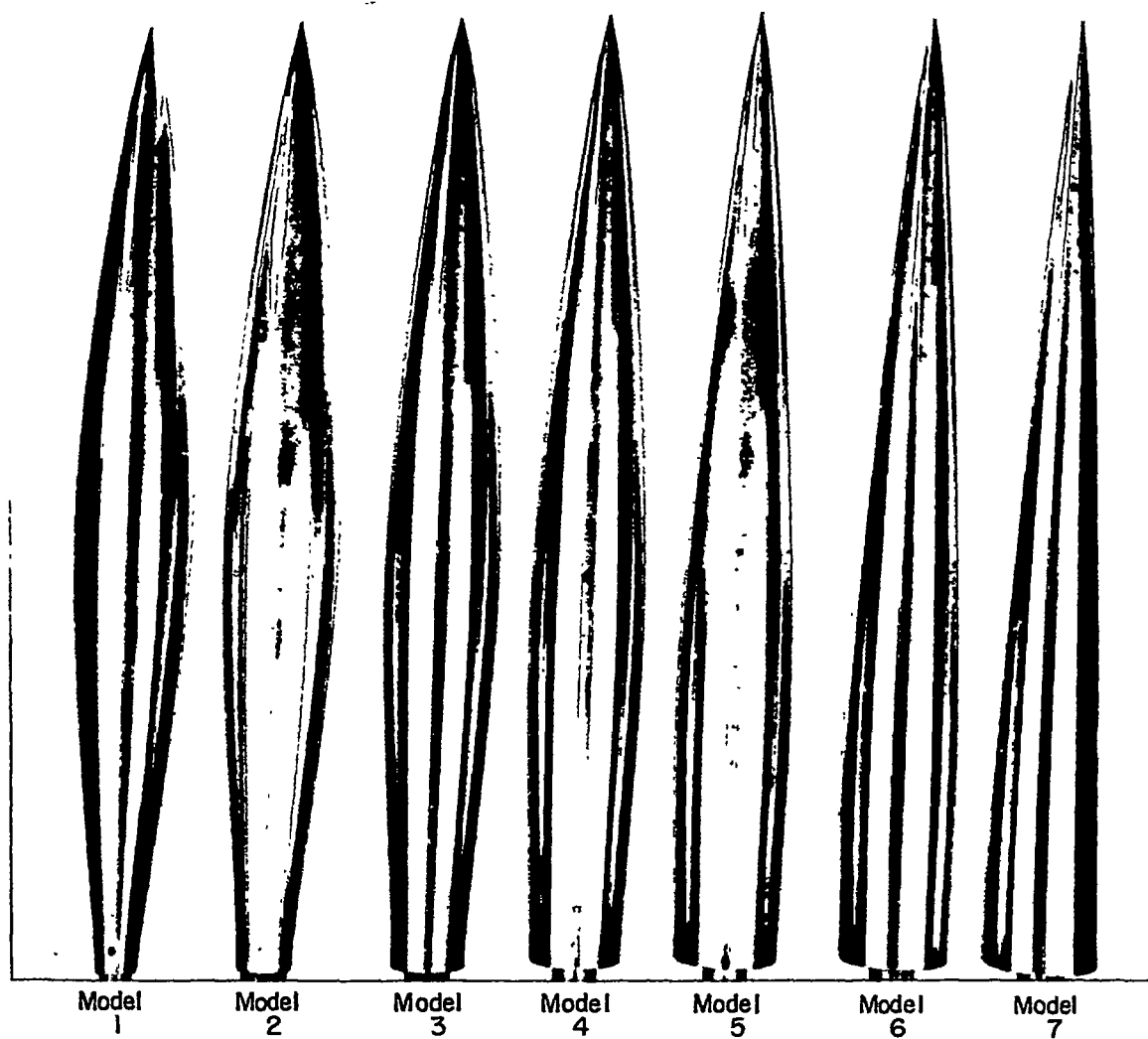


Figure 1.- Drawing of models. All dimensions are in inches.



L-80240

Figure 2.- Photograph of models.

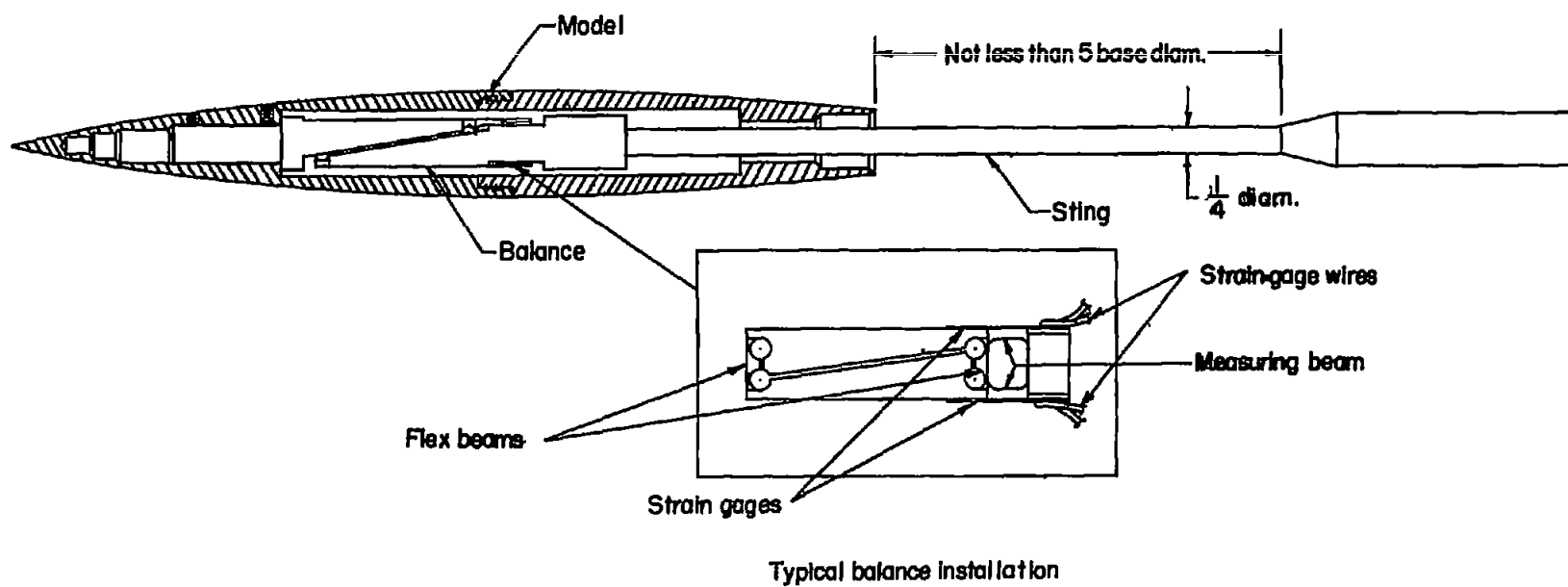


Figure 3.- Wire strain-gage balance.

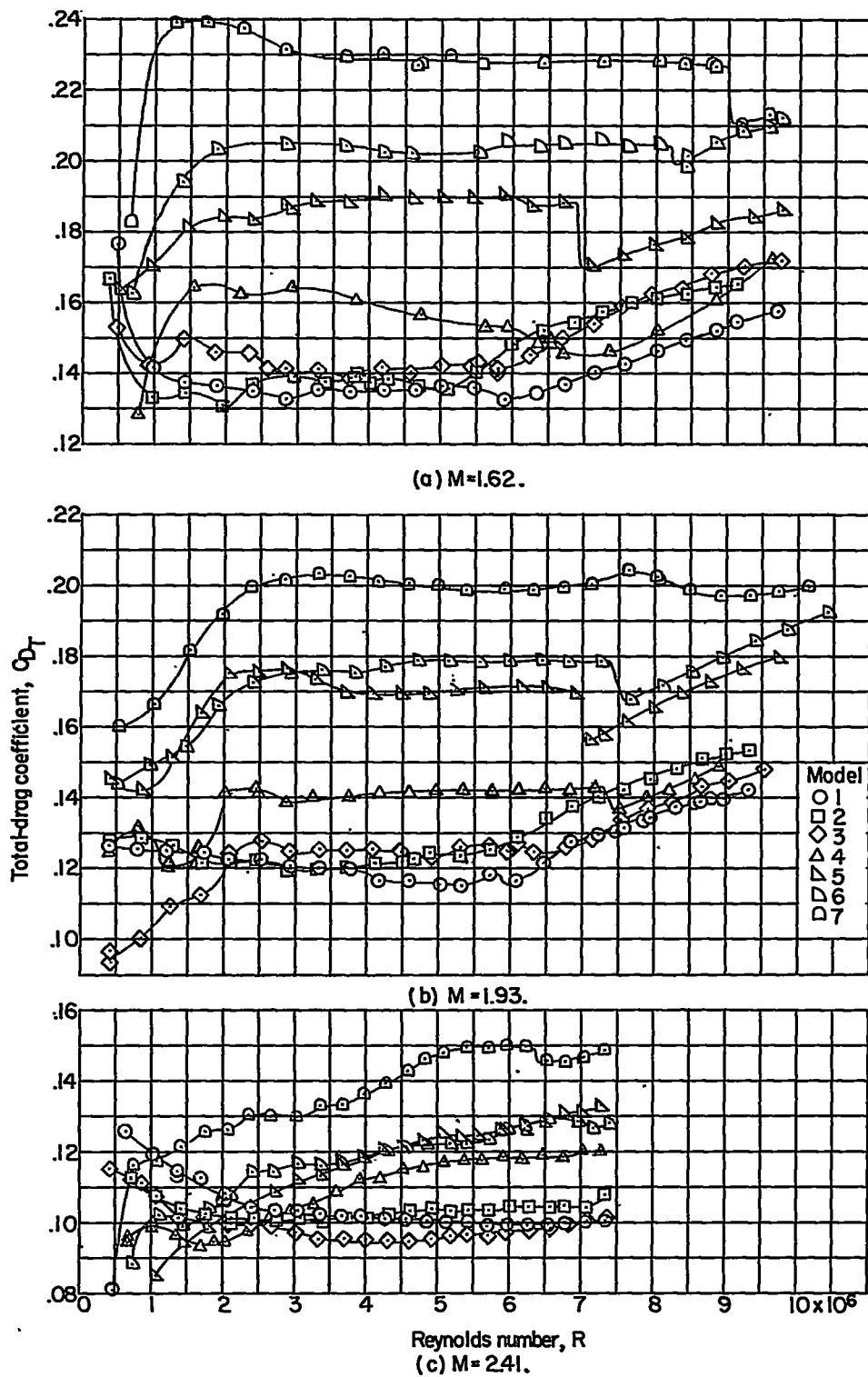


Figure 4.- Variation of total-drag coefficient with Reynolds number at  $M = 1.62, 1.93$ , and  $2.41$ .

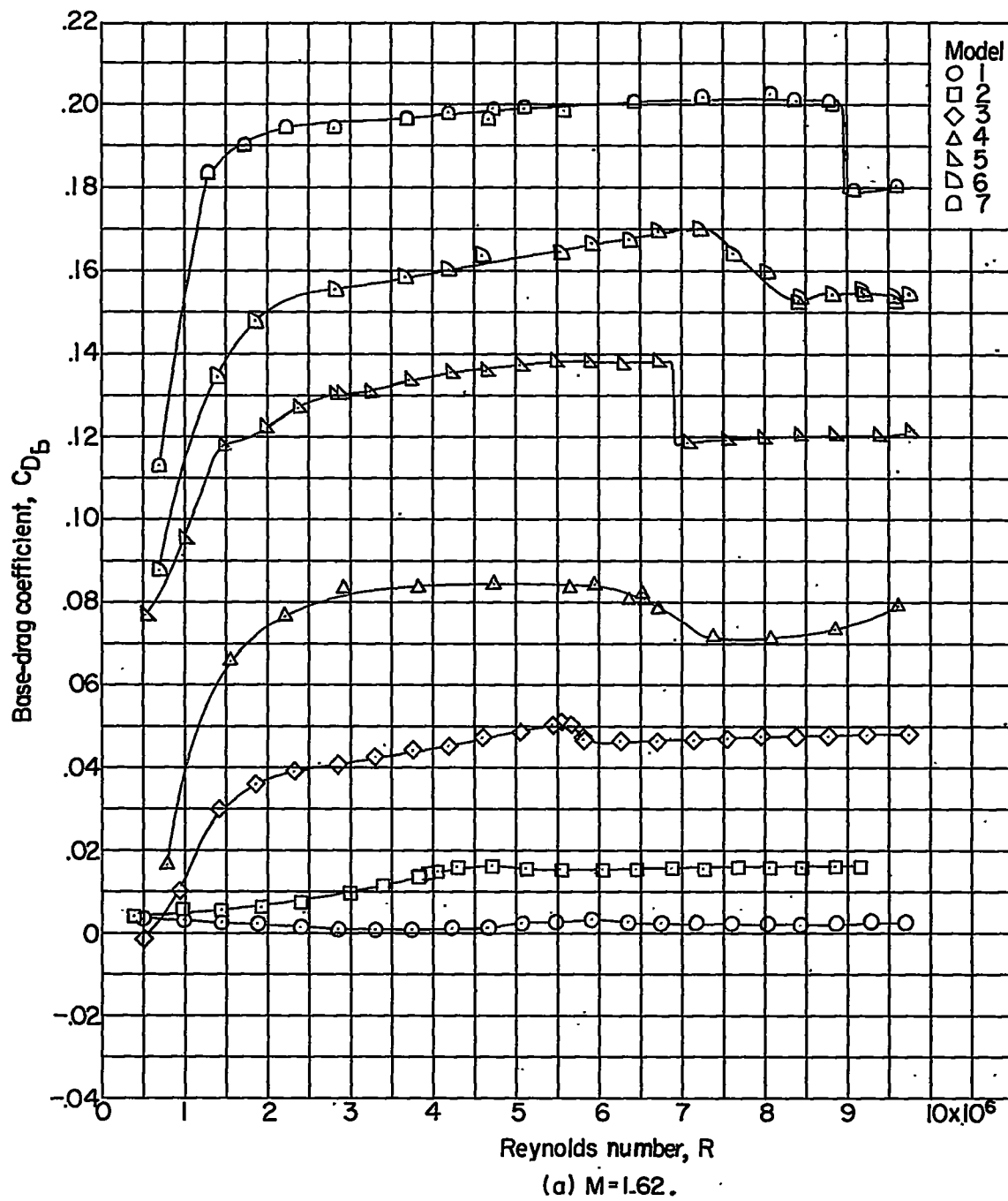


Figure 5.- Variation of base-drag coefficient with Reynolds number.



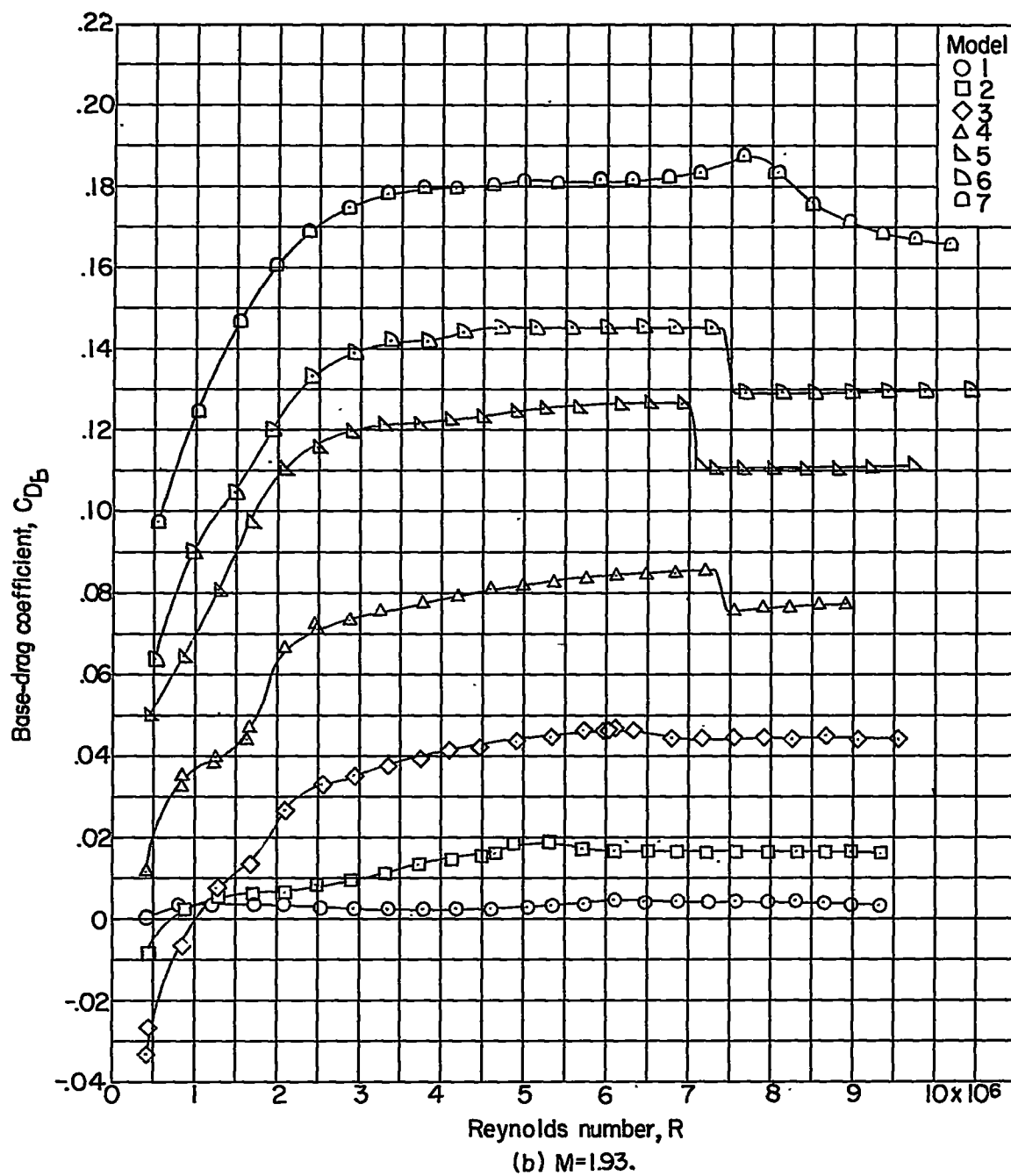


Figure 5.- Continued.

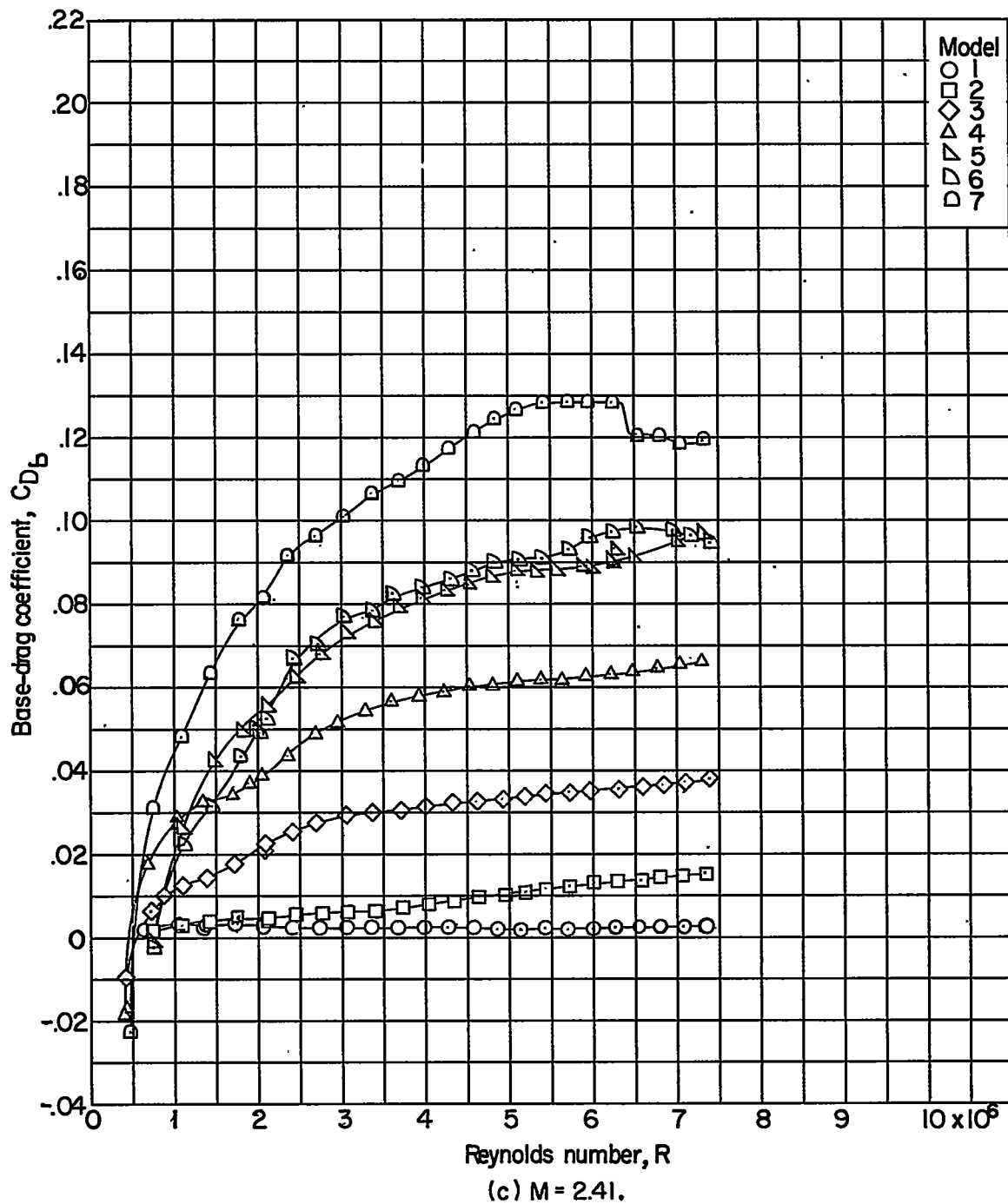


Figure 5:- Concluded.

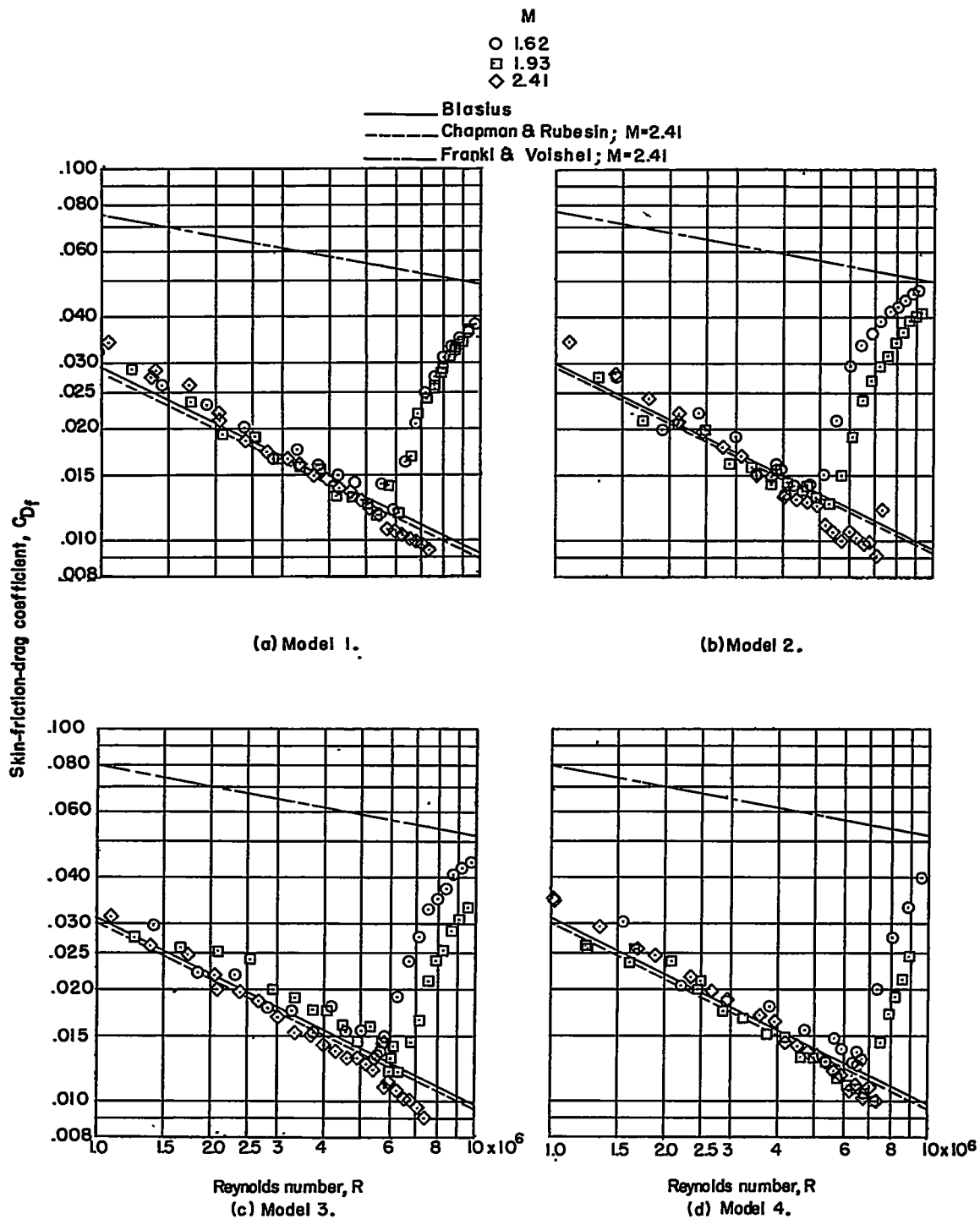


Figure 6.- Variation of skin-friction-drag coefficient with Reynolds number at  $M = 1.62$ ,  $1.93$ , and  $2.41$ .

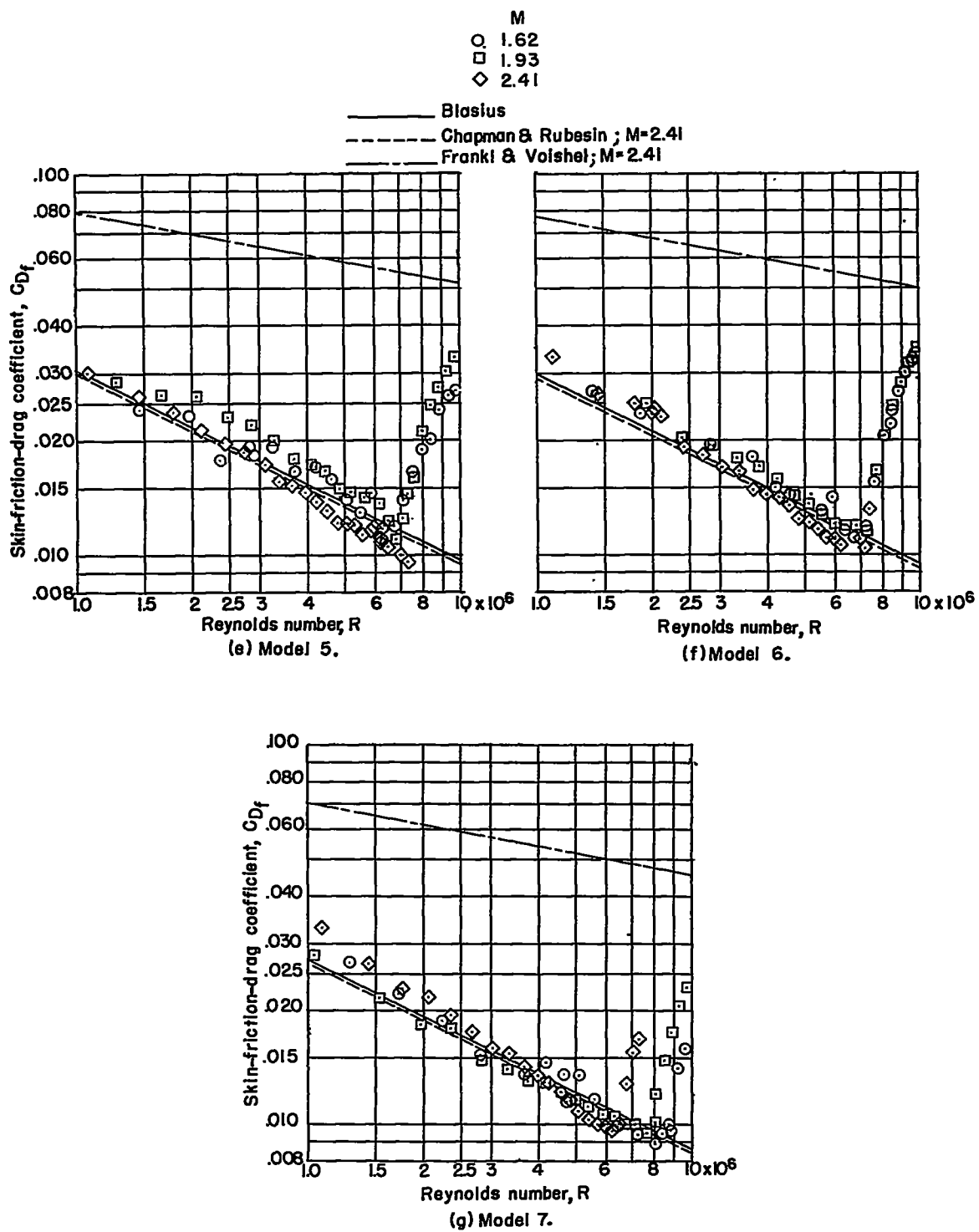


Figure 6.- Concluded.

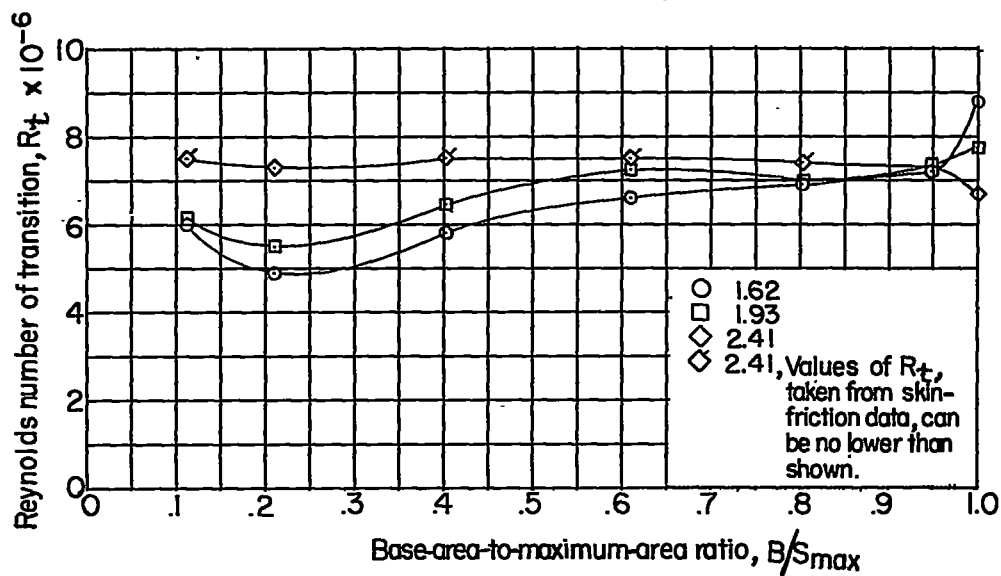


Figure 7.- Variation of Reynolds number of transition with ratio of base area to maximum area at  $M = 1.62$ ,  $1.93$ , and  $2.41$ .

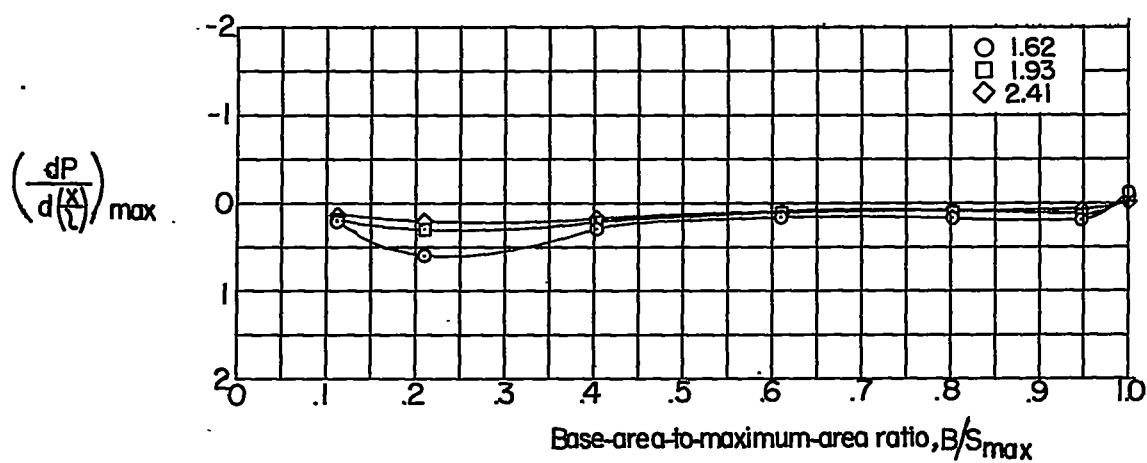


Figure 8.- Variation of maximum adverse pressure gradient with ratio of base area to maximum area at  $M = 1.62$ ,  $1.93$ , and  $2.41$ .